Sciencexpress Research Article

# Control Mechanism of the Circadian Clock for Timing of Cell Division in Vivo

Takuya Matsuo,[1,2]* Shun Yamaguchi,[1]* Shigeru Mitsui,[1] Aki Emi,[1] Fukuko Shimoda,[1] Hitoshi Okamura[1]†

[1]Division of Molecular Brain Science, Department of Brain Sciences, Kobe University Graduate School of Medicine, Chuo-ku, Kobe 650-0017, Japan. [2]Department of Physics, Informatics and Biology, Yamaguchi University, Yamaguchi 753-8512, Japan.

*These authors contributed equally to this work.

†To whom correspondence should be addressed. E-mail: okamurah@kobe-u.ac.jp

**Cell division in many mammalian tissues is associated with specific times of day but just how the circadian clock controls this timing has not been clear. Here we show in the regenerating liver (of mice) that the circadian clock controls the expression of cell cycle-related genes that in turn, modulate the expression of active Cyclin B1-Cdc2 kinase, a key regulator of mitosis. Among these genes, expression of *wee1* was directly regulated by the molecular components of the circadian clockwork. In contrast, the circadian clockwork oscillated independently of the cell cycle in single cells. Thus, the intracellular circadian clockwork can control the cell division cycle directly and unidirectionally in proliferating cells.**

Circadian (~24-hr) rhythms and cell division are fundamental biological systems in most organisms. There is substantial evidence that in mammals, circadian rhythms affect the timing of cell divisions *in vivo*. Day-night variations in both the mitotic index and DNA synthesis occur in many tissues (*e.g.* oral mucosa, tongue keratinocytes, intestinal epithelium, skin, and bone marrow)(*1–6*), some of which persist even in constant darkness (*7*). However, how the circadian clock controls the timing of cell divisions is not known.

To explore the relationship between cell division and circadian rhythms, we used a mouse model with partial hepatectomy (PH)(*8–13*). After a 2/3 partial hepatectomy (*14*), most of the remaining hepatocytes rapidly and simultaneously enter into the cell cycle, resulting in restoration of the liver mass in a few days.

**Diurnal control of cell cycle in wild-type mice.** PH was performed on mice (*15*) at ZT8 or ZT0 (ZT, Zeitgeber time in a 12hr light-12hr dark cycle; ZT0 represents lights-on and ZT12 lights-off) to compare the kinetics of subsequent cell cycles. The kinetics of S-phase (DNA-synthesizing) hepatocytes for both ZTs were comparable as determined by bromodeoxyuridine (BrdU) incorporation into nuclei, peaking at 36 hr after PH (Fig. 1A). In contrast, subsequent mitotic waves were differed (Fig. 1B). When PH was performed at ZT8 (PH/ZT8), a massive entry of hepatocytes into the M phase occurred within 40 hr after PH. In the case of PH/ZT0, however, only a few cells entered the M phase within 44 hr and a mitotic peak was reached 48 hr after PH. These results suggest that the time of operation has a marked effect on the timing of mitosis controlling the progression of cell cycling itself.

To investigate the molecular mechanism underlying this time- of-day-dependent regulation of the cell cycle, the kinase activity of Cdc2 (*15*), an initiator of mitosis (*16*), was examined. Peaks of Cdc2 activity after PH/ZT8 and PH/ZT0 occurred 40 hr and 48 hr after PH, respectively, corresponding to the observed mitotic peaks (Fig. 1B, C). This suggests that the regulation of the expression of the active Cdc2 kinase is an important process for the diurnal control of the cell cycle.

Analysis of the expression profiles of 68 cell cycle-related genes by DNA microarray and Northern blot analysis (fig. S1A, B; fig. S2; table S1), revealed that while 11 genes showed moderately different kinetics between PH/ZT8 and PH/ZT0 (differences of 1.5 to 2.2-fold or 0.67 to 0.42-fold; ratios of PH/ZT0 to PH/ZT8)(fig. S2; table S2), only three genes, *cyclin B1*, *cdc2*, and *wee1*, showed remarkably different expression profiles (a difference of more than 2.7-fold) between 28 and 56 hr after PH (Fig. 1D).

The expression peaks of *cyclin B1* and *cdc2* transcripts, whose products form Cyclin B1-Cdc2-complex kinase, corresponded with Cdc2 kinase activity peaks (Fig. 1C, D). Both mRNA peaks were delayed by 8 to 12 hrs after PH/ZT0 compared to PH/ZT8. As for the *wee1* gene, whose product phosphorylates Cdc2 on Tyr-15 [p-Cdc2(Tyr 15)] and keeps it in an inactive form (*17*, *18*), decrease of its mRNA corresponded with the increase of the Cdc2 kinase activity (Fig. 1C, D) with the same time delay. These results suggest that the transcript level regulation of *cyclin B1*, *cdc2*, and *wee1* contributes to the timing of entry into mitosis.

**Impaired liver regeneration in arrhythmic *Cry*-deficient mice.** Mice that lack the clock regulator *cryptochromes* (*Crys*) completely lack free-running rhythmicity. Yet, embryogenesis and postnatal development in these mice appear normal (*19*) suggesting that clock function is not absolutely required for cell cycling. Although the mean weight of the pre-PH livers of wild-type (WT) and *Cry*-deficient animals was the same ($P>0.05$), the weight of the regenerating liver in *Cry*-deficient mice 72 hr after PH/ZT8 was significantly lower than that of WT mice (53.1±3.0% and 64.1±1.7% of pre-PH liver weight, respectively; Student's *t*-test, $P<0.05$) (Fig. 2A). This value of *Cry*-deficient mice was also lower than that of WT mice 72 hr after PH/ZT0 (66.4±1.7%; $P<0.01$), suggesting impairment of hepatocyte proliferation in *Cry*-deficient mice. However, in both genotypes, liver weight returned to pre-PH levels by day

10 (Fig. 2A) and histological analyses (including comparisons of the number and cell size of hepatocytes, and average distances separating portal and central hepatic veins), did not reveal any major differences (*20*). This indicates that circadian clock function is required for efficient cell cycling *in vivo*.

The kinetics of S-phase hepatocytes following PH/ZT8 or PH/ZT0 in *Cry*-deficient and WT mice were comparable (Fig. 2B). However, in the subsequent mitotic wave, the maximum value of mitotic hepatocytes was low (less than 4% for both PH/ZT8 and PH/ZT0)(Fig. 2B). Furthermore, Cdc2 kinase activity was reduced (Fig. 2B, 1C). Therefore, the cell cycle progression from S- to M-phase was impaired during liver regeneration in *Cry*-deficient mice. In addition, because *Cry*-deficient mice did not exhibit a mitotic wave that depended on the time of operation, functional impairment of the control mechanism for mitotic timing *in vivo* is indicated.

To determine the molecular mechanism underlying the failure to progress through the cell cycle in *Cry*-deficient mice, the expression profiles of the cell cycle-related genes were compared between WT and *Cry*-deficient mice (fig. S1C, D; fig. S3; table S1, S3). After PH/ZT8, seven of 68 analyzed genes showed different expression profiles: Differences of a more than 2.7-fold or less than 0.37-fold (ratios of *Cry*-deficient to WT) were observed between 32 and 56 hr after PH (Fig. 2C). These included the M-phase-related genes *cyclin B1*, *cdc2*, *wee1*, *Bub1*, and *p55CDC,* the S-phase and M-phase-related gene *cyclin A2*, and the G1-phase-related gene *cyclin D1* (*21*). In *Cry*-deficient mice, the expression peaks of *cyclin B1*, *cdc2*, *Bub1*, *p55CDC*, and *cyclin A2* occurred 8-12 hr later than those in WT mice, corresponding to the peak mitotic timing (48 hr after PH) (Fig. 2B, C). The expression profiles of *cyclin D1* and *wee1* transcripts were markedly different between *Cry*-deficient and WT mice throughout the liver regeneration process: *cyclin D1* expression decreased up to 86% and *wee1* expression increased up to 4.6-fold between 32 and 72 hr after PH (Fig. 2C). These results indicate that the expression of many cell cycle-related genes is deregulated in *Cry*-deficient mice, and underlies impairment of cell cycle progression.

**Direct regulation of *wee1* transcription by circadian clockwork.** We further focused our attention on the *wee1* gene because [1] the expression pattern of *wee1* during liver regeneration in *Cry*-deficient mice and its circadian cycling in normal mouse liver (*22*, *23*), raised the possibility that *wee1* transcription may be directly driven by the circadian oscillatory machinery, and [2] it had been known that the expression level of WEE1 profoundly affects the timing of M phase entry in mammalian cells (*18*, *24*, *25*). In normal mouse livers, *wee1* mRNA displayed a robust circadian oscillation showing a 22.8-fold amplitude with a peak at circadian time (CT)8 (where CT0 is subjective dawn and CT12 is subjective dusk) (Fig. 3A). In *Cry*-deficient mice, *wee1* mRNA levels were high at both ZT0 and ZT12. However in *Clock* mutant (*Clock/Clock*) mice (*26*), which carry dominant-negative *Clock* mutations (*27*), *wee1* expression was low at both ZTs (Fig. 3A). These expression profiles correspond to the notion that the *wee1* transcription is regulated by the molecular components of the circadian clock: activated by CLOCK/BMAL1 heterodimers (*27*) and suppressed by PER/CRY proteins (*28*).

The CLOCK-BMAL1 complex acts on E-box elements of target genes. Three E-box (CACGTG) elements were found within 1.2-kb of the mouse *wee1* gene 5'-upstream region (Fig. 3B). CLOCK and BMAL1 together, but neither of them alone, produced a major increase in transcriptional activity via this fragment in transfected NIH3T3 cells (52.7-fold; Student's *t*-test, $P<0.001$) (Fig. 3C). This activation was drastically reduced when all three E-boxes were mutated (82.6%; $P<0.001$) (Fig. 3C). PER1, PER2, and PER3 moderately reduced (32.1%, 71.8%, and 21.8%, respectively; $P<0.05$), and CRY1 and CRY2 completely abolished the CLOCK-BMAL1-induced transcription (Fig. 3C). These results suggest that the *wee1* transcription is directly regulated by the core components of the feedback loop of the circadian oscillatory mechanism.

During liver regeneration, *wee1* mRNA levels in WT mice were high between ZT8 and 16, and low around ZT0 (Fig. 1D), similar to unoperated mice (Fig. 3A). In *Cry*-deficient mice, *wee1* mRNA levels were elevated throughout regeneration (Fig. 2C) whereas they were low in *Clock/Clock* mice (Fig. 3D). These results suggest that the direct regulation by the circadian clockwork is maintained even during the regeneration process.

We next examined whether the fluctuations in the quantities of *wee1* mRNA are reflected in WEE1 protein and kinase activity levels in regenerating livers. In WT mice, the peaks of WEE1 protein expression occurred 36 hr after PH/ZT8 and 40–44 hr after PH/ZT0, 4–8 hr before the corresponding mitotic peaks (Fig. 3E)(*15*). Subsequently, the WEE1 protein levels rapidly decreased in both groups (Fig. 3E). These expression profiles were closely reflected by changes in the WEE1 kinase activity (Fig. 3F)(*15*). In *Cry*-deficient mice, WEE1 protein levels and WEE1 kinase activity were very high between 32 and 52 hr after PH (Fig. 3E, F). These results suggest that the fluctuations in the quantity of *wee1* mRNA are reflected in the WEE1 protein and kinase activity levels in regenerating livers.

We next examined the kinetics of the phosphorylation of Cdc2 on Tyr-15, which is predominantly carried out by the WEE1 kinase (*17*, *18*). In WT mice, the p-Cdc2(Tyr 15) levels reached a peak 36-40 hr after PH/ZT8 and 44–48 hr after PH/ZT0 (Fig. 3G)(*15*). Thus, the peak expression for both ZTs was about 4 hr later than that of the corresponding WEE1 kinase activity. However, when the total amount of Cdc2 protein during liver regeneration was taken into account (Fig. 3G) and the ratios of p-Cdc2(Tyr 15) to Cdc2 were calculated, the peak times for both ZTs corresponded well with the WEE1 kinase activity peaks (Fig. 3F, G). These peaks occurred 4 hr before the corresponding Cdc2 kinase activity peaks (Fig. 1C). In *Cry*-deficient mice, both the amount of p-Cdc2(Tyr 15) and the p-Cdc2(Tyr 15)/Cdc2 ratios were high between 32 and 52 hr after PH (Fig. 3G). This, at least in part, accounts for the low activity of the Cdc2 kinase in *Cry*-deficient mice (Fig. 2B). The increase in p-Cdc2(Tyr 15) is thought to be due to the high level of WEE1 kinase expression because Myt1, another Cdc2(Tyr 15)

phosphorylating kinase (*29*), showed no significant difference in the quantities of mRNA and protein between WT and *Cry*-deficient mice (fig. S4). Taken together, it is suggested that the fluctuations in the quantities of *wee1* mRNA are closely reflected by its protein and kinase activity, target phosphorylation, and Cdc2 kinase activity. Thus, the circadian clock-*wee1* pathway functions as a vital means of controlling the cell cycle *in vivo*.

**Functional clock in dividing hepatocytes.** To determine whether the circadian clock continues to function during the massive entry of hepatocytes into the cell cycle, expression profiles of clock components, *Per1*, *Per2*, *Cry1*, and *Bmal1* were examined. Robust oscillations in these mRNAs with a periodicity of 24 hr (fig. S5A, B), were observed in WT unoperated mice. After PH/ZT8 or PH/ZT0, these expression profiles were mostly conserved, even on the first day after PH (fig. S5A, B). At the same time, more than 70% hepatocytes (71.0±6.2% for PH/ZT8 and 70.1±0.7% for PH/ZT0) were involved in cell cycling on the second day (fig. S5C). These results suggest that the intrinsic circadian clock continued to function in the regenerating liver even when the majority of the hepatocytes were going through the cell cycle.

At the single cell level, PER2 protein expression in hepatocyte nuclei as determined by immunohistochemistry (*15*), was observed in the livers of unoperated mice at ZT20, 4 hr after the *Per2* mRNA peaks (Fig. 4A). No cytoplasmic or nuclear PER2 was found between ZT0 and ZT16. PER2 immunoreactivity in nonparenchymal cells, including endothelial, Kupffer, and ductal cells, was below the level of detection at all times (*20*). After PH/ZT8, nuclear PER2 was found again at exactly ZT20 (12, 36, and 60 hr after PH)(Fig. 4B). Moreover, PER2 accumulated in nuclei of BrdU-stained cells, exactly as in unstained cells (Fig. 4B). This was also observed after PH/ZT0 (fig. S6). Therefore, the circadian clockwork oscillated accurately in a single proliferating cell. Furthermore, the circadian output genes *dbp*, *hlf*, *tef*, *e4bp4*, and *cyp7a*, displayed robust oscillations in their transcript expression levels throughout the regeneration process (fig. S7), indicating that the intracellular circadian clockwork is functional and is able to control the timing of the cell cycle-related gene expression during the regenerating process.

Finally, we investigated whether the circadian rhythms of the clock gene expression persist in proliferating hepatocytes in the absence of cell cycling. Prior to partial hepatectomy performed at ZT8, the mice were given retrorsine (*15*), which inhibits hepatocyte cell division for several weeks (*30*). This treatment resulted in a cell cycle block that allowed DNA synthesis but almost completely eliminated the subsequent mitotic division (the highest value of the mitotic index between 36 to 64 hr after PH was less than 0.2%) (fig. S8A). Even under these conditions, PER2 expression was still observed in almost all hepatocytes (99.1% of 2000 cells) at exactly ZT20 (36 and 60 hr after PH) (fig. S8B), indicating that the circadian oscillatory mechanism in proliferating hepatocytes did not require the help of cell cycle for its normal functioning.

**Conclusion and perspective.** We have observed that the circadian clockwork can oscillate accurately and independently of the cell cycle in proliferating hepatocytes, and that this intrinsic oscillatory mechanism may participate in regulating the timing and efficiency of cell cycle events through clock-controlled genes such as *wee1*. Although external humoral and/or neural timing cues may also participate in cell-cycle regulation (*12*), the presence of intracellular pathways from the circadian clockwork to the cell cycle system indicates a strong correlation of the timing of clock gene expression with the timing of cell cycle events in not only regenerating liver but also continuously proliferating tissues (*e.g.* oral and gastrointestinal mucosa, skin, and bone marrow). Although only a few studies have examined both clock gene expression and cell-cycle events simultaneously in proliferating tissues (*31*), the following relationship may be conserved: Expression of *wee1* is high when the transcript of *Per1*, another CLOCK-BMAL1-driven gene, is abundant in these tissues, and the entry into the M phase is suppressed during that time of day. Our findings give a new viewpoint on cell-cycle research. Furthermore, because the circadian phase-dependent toxicity and antitumor effects of several chemotherapy drugs have been reported (*32*), our findings may help to improve and refine the therapeutic strategies.

**References and Notes**


1. G.A. Bjarnason, R. Jordan, *Prog. Cell Cycle Res.* **4,** 193 (2000).
2. M.N. Garcia, C.G. Barbeito, L.A. Andrini, A.F. Badran, *Cell Biol. Int.* **25,** 179 (2001).
3. L.E. Scheving, T.H. Tsai, L.A. Scheving, *Am. J. Anat.* **168,** 433 (1983).
4. K.N. Buchi, J.G. Moore, W.J. Hrushesky, R.B. Sothern, N.H. Rubin, *Gastroenterology* **101,** 410 (1991).
5. W.R. Brown, *J. Invest. Dermatol.* **97,** 273 (1991).
6. R. Smaaland, *Prog. Cell Cycle Res.* **2,** 241 (1996).
7. L.E. Scheving, J.E. Pauly, H. von Mayersbach, J. D. Dunn, *Acta Anat.* **88,** 411 (1974).
8. J.J. Jaffe, *Anat. Rec.* **120,** 935 (1954).
9. C.P. Barnum, C.D. Jardetsky, F. Halberg, *Texas Rep. Biol. Med.* **15,** 134 (1957).
10. E.G. Bade, I.L. Sadnik, C. Pilgrim, W. Maurer, *Exp. Cell Res.* **44,** 676 (1966).
11. M. Souto, J.M. Llanos, *Chronobiol. Int.* **2,** 169 (1985).
12. H. Barbason *et al.*, *In Vivo* **9,** 539 (1995).
13. B. Barbiroli, V.R. Potter, *Science* **172,** 738 (1971).
14. G.M. Higgins, R.M. Anderson, *Arch. Pathol.* **12,** 186 (1931).
15. Materials and methods are available as supporting material on *Science* Online.
16. R. Ohi, K.L. Gould, *Curr. Opin. Cell Biol.* **11,** 267 (1999).
17. L.L. Parker, H. Piwnica-Worms, *Science* **257,** 1955 (1992).
18. C.H. McGowan, P. Russell, *EMBO J.* **12,** 75 (1993).
19. G.T.J. van der Horst *et al.*, *Nature* **398,** 627 (1999).
20. T. Matsuo, unpublished data.
21. J. Pines, *Nat. Cell Biol.* **1,** E73 (1999).
22. R.A. Akhtar *et al.*, *Curr. Biol.* **12,** 540 (2002).
23. K.F. Storch *et al.*, *Nature* **417,** 78 (2002).

24. C.J. Rothblum-Oviatt, C.E. Ryan, H. Piwnica-Worms, *Cell Growth Differ.* **12,** 581 (2001).
25. R. Heald, M. McLoughlin, F. McKeon, *Cell* **74,** 463 (1993).
26. D.P. King *et al*., *Cell* **89,** 641 (1997).
27. N. Gekakis *et al*., *Science* **280,** 1564 (1998).
28. K. Kume *et al.*, *Cell* **98,** 193 (1999).
29. F. Liu, J.J. Stanton, Z. Wu, H. Piwnica-Worms, *Mol. Cell. Biol.* **17,** 571 (1997).
30. S. Laconi *et al.*, *J. Hepatol.* **31,** 1069 (1999).
31. G.A. Bjarnason *et al.*, *Am. J. Pathol.* **158,** 1793 (2001).
32. F. Levi, *Chronobiol. Int.* **19,** 1 (2002).
33. H. Kawasaki *et al*., *EMBO J.* **20,** 4618 (2001).
34. The authors wish to thank M. Iwai (Kyoto Prefectural University of Medicine) for advising the technique of hepatectomy; G.T.J. van der Horst (Erasmus University) for providing access to *Cry*-deficient mice; and A. Ishida and T. Okamoto (Kobe University) for technical assistance. This work was supported in part by grants from the Special Coordination Funds, the Grant-in-Aid for the Scientific Research on Priority Areas of the Ministry of Education, Culture, Sports, Science and Technology of Japan, the Kanae Foundation for Life and Socio-medical Science, and the Inamori Foundation.

**Supporting Online Material**
www.sciencemag.org/cgi/content/full/1086271/DC1
Materials and Methods
References
Tables S1 to S3
Figs. S1 to S8

29 April 2003; accepted 8 August 2003
Published online 21 August 2003; 10.1126/science.1086271
Include this information when citing this paper.

**Fig. 1.** Effects of time of PH on subsequent liver regeneration. **A**, Kinetics of DNA synthesis (BrdU-incorporation) in hepatocytes after PH/ZT8 and PH/ZT0. Values show mean percentage ± s.e.m. in 2000 nuclei per animal. **B**, Kinetics of mitotic hepatocytes after PH/ZT8 and PH/ZT0. Values in the graph show mean percentage ± s.e.m. in 3000 hepatocytes per animal. **C,** Kinetics of Cdc2 kinase activity after PH/ZT8 and PH/ZT0. Cdc2 was immunoprecipitated from liver lysates and its kinase activity was determined by an *in vitro* kinase assay with histone H1 as the substrate. The peak value for the PH/ZT8 mice was adjusted to 100. **D**, Temporal expression profiles of *cyclin B1*, *cdc2*, and *wee1* mRNAs after PH/ZT8 and PH/ZT0. Northern blot analyses for total RNAs (20 μg) isolated from the livers of operated mice are shown at the top. Quantified relative mRNA levels are shown in the graphs. The peak values for the PH/ZT8 mice were adjusted to 100. No variations were detected in the amounts of mRNA loaded as the result of hybridization with an *albumin* cDNA probe. White and black bars above the graphs represent times when lights were on or off, respectively (**A**-**D**). Scale bar, 30 μm (**A, B**).

**Fig. 2.** Liver regeneration in *Cry*-deficient mice. **A**, Liver weights of WT (PH/ZT8 and PH/ZT0) and *Cry*-deficient (PH/ZT8) mice 72 hr and 10 days after PH. Pre-PH liver weight (removed liver weight x 1/0.67) of the animals was adjusted to 100%. Values represent the mean ± s.e.m. (n=4 to 6). Single and double asterisks denote statistically significant differences ($P<0.01$ and $P<0.05$, respectively). **B**, Kinetics of BrdU-stained hepatocytes (top), mitosis (middle), and Cdc2 kinase activity (bottom) in *Cry*-deficient mice after PH. Values in the top and middle graphs were determined as in Fig. 1A and B. In the bottom graph, relative values were calculated setting the peak value for PH/ZT8 in Fig. 1C as 100. **C**, Temporal expression profiles of the cell cycle-related genes that showed markedly different expression patterns between WT and *Cry*-deficient mice after PH. Northern blot analyses for the regenerating livers after PH/ZT8 are shown as in Fig. 1D. The peak values for the WT mice were adjusted to 100.

**Fig. 3.** Circadian regulation of the *wee1* gene at the mRNA, protein, and kinase activity levels. **A**, Expression pattern of *wee1* in WT, *Cry*-deficient, and *Clock/Clock* mice. Northern blot analysis results for total RNAs (10 μg) isolated from unoperated mouse livers are shown. **B,** Location of the E-box sites within the 5'-flanking region of the mouse *wee1* gene. The arrow indicates the transcription start site (*33*). **C**, Transcriptional regulation of the mouse *wee1* gene by clock genes. Reporter plasmid containing the 1.2-kb mouse *wee1* 5'-upstream region, including the three E-boxes (*wee1* 1.2-kb) or mutated E-boxes (all three E-boxes were mutated to 5'-CTGCAG-3'; mutant 1.2-kb), was used for the transcriptional assay. Presence (+) or absence (–) of the reporter and expression plasmids is shown. Each value represents the mean ± s.e.m. of three replicates for a single assay. These results are representative of at least three independent experiments. **D**, *wee1* expression levels in *Clock/Clock* mice after PH/ZT8. The expression profiles in WT (broken blue line) and *Cry*-deficient mice (broken red line) are superimposed for comparison. **E,** WEE1 protein levels in WT (PH/ZT8 and PH/ZT0) and *Cry*-deficient mice (PH/ZT8). WEE1 protein was immunoprecipitated from liver lysates and its amounts were analyzed by immunoblot analysis. **F,** WEE1 kinase activity in WT (PH/ZT8 and PH/ZT0) and *Cry*-deficient mice (PH/ZT8). Immunoprecipitated WEE1 was used for the *in vitro* kinase assay with Cyclin B1-Cdc2 as substrate. The phosphorylation of Cdc2 on Tyr-15 was assessed by immunoblot analysis with an anti-p-Cdc2(Tyr 15)-specific antibody. The peak values for the WT PH/ZT8 mice were adjusted to 100 (**D**-**F**). **G,** Kinetics of p-Cdc2(Tyr 15), Cdc2, and their ratios. Cdc2 was immunoprecipitated from liver lysates and its amounts were analyzed by immunoblot analysis (middle). The same immunoprecipitates were used for determining the amounts of p-Cdc2(Tyr 15) by immunoblot analysis with the anti- p-Cdc2(Tyr 15)-specific antibody (top). The peak values for the WT PH/ZT8 mice were adjusted to 100 (top and middle). Each value in the top graph was simply divided by the corresponding middle graph value (bottom).

**Fig. 4.** PER2 protein expression in proliferating hepatocytes. **A**, Immunofluorescence analysis (red) showing the temporal expression profile of PER2 protein in unoperated control

livers. Nuclei were counterstained with DAPI (blue). **B**, Nuclear PER2 accumulation (red) in BrdU-stained (green) and unstained hepatocytes at regular time intervals after PH/ZT8. Scale bar, 30 μm (**A, B**).

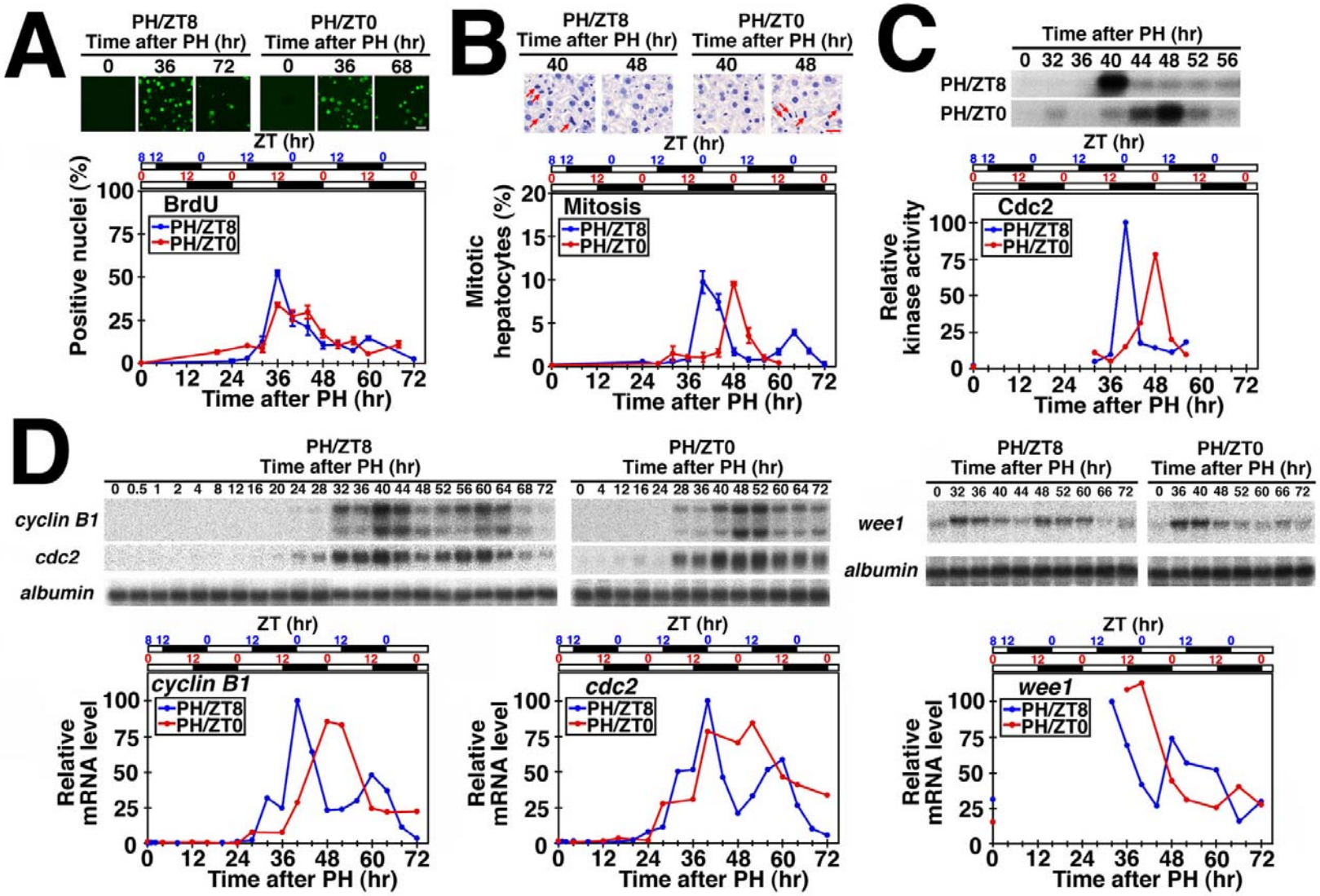
A
PH/ZT8
Time after PH (hr)
0 36 72
PH/ZT0
Time after PH (hr)
0 36 68
ZT (hr)
8 12 0 12 0 12 0
0 12 0 12 0 12 0
BrdU
PH/ZT8
PH/ZT0
Positive nuclei (%)
100
75
50
25
0
0 12 24 36 48 60 72
Time after PH (hr)
B
PH/ZT8
Time after PH (hr)
40 48
PH/ZT0
Time after PH (hr)
40 48
ZT (hr)
8 12 0 12 0 12 0
0 12 0 12 0 12 0
Mitosis
PH/ZT8
PH/ZT0
Mitotic hepatocytes (%)
20
15
10
5
0
0 12 24 36 48 60 72
Time after PH (hr)
C
Time after PH (hr)
0 32 36 40 44 48 52 56
PH/ZT8
PH/ZT0
ZT (hr)
8 12 0 12 0 12 0
0 12 0 12 0 12 0
Cdc2
PH/ZT8
PH/ZT0
Relative kinase activity
100
75
50
25
0
0 12 24 36 48 60 72
Time after PH (hr)
D
PH/ZT8
Time after PH (hr)
0 0.5 1 2 4 8 12 16 20 24 28 32 36 40 44 48 52 56 60 64 68 72
PH/ZT0
Time after PH (hr)
0 4 12 16 24 28 36 40 48 52 60 64 72
cyclin B1
cdc2
albumin
PH/ZT8
Time after PH (hr)
0 32 36 40 44 48 52 60 66 72
PH/ZT0
Time after PH (hr)
0 36 40 48 52 60 66 72
wee1
albumin
ZT (hr)
8 12 0 12 0 12 0
0 12 0 12 0 12 0
cyclin B1
PH/ZT8
PH/ZT0
Relative mRNA level
100
75
50
25
0
0 12 24 36 48 60 72
Time after PH (hr)
ZT (hr)
8 12 0 12 0 12 0
0 12 0 12 0 12 0
cdc2
PH/ZT8
PH/ZT0
Relative mRNA level
100
75
50
25
0
0 12 24 36 48 60 72
Time after PH (hr)
ZT (hr)
8 12 0 12 0 12 0
0 12 0 12 0 12 0
wee1
PH/ZT8
PH/ZT0
Relative mRNA level
100
75
50
25
0
0 12 24 36 48 60 72
Time after PH (hr)

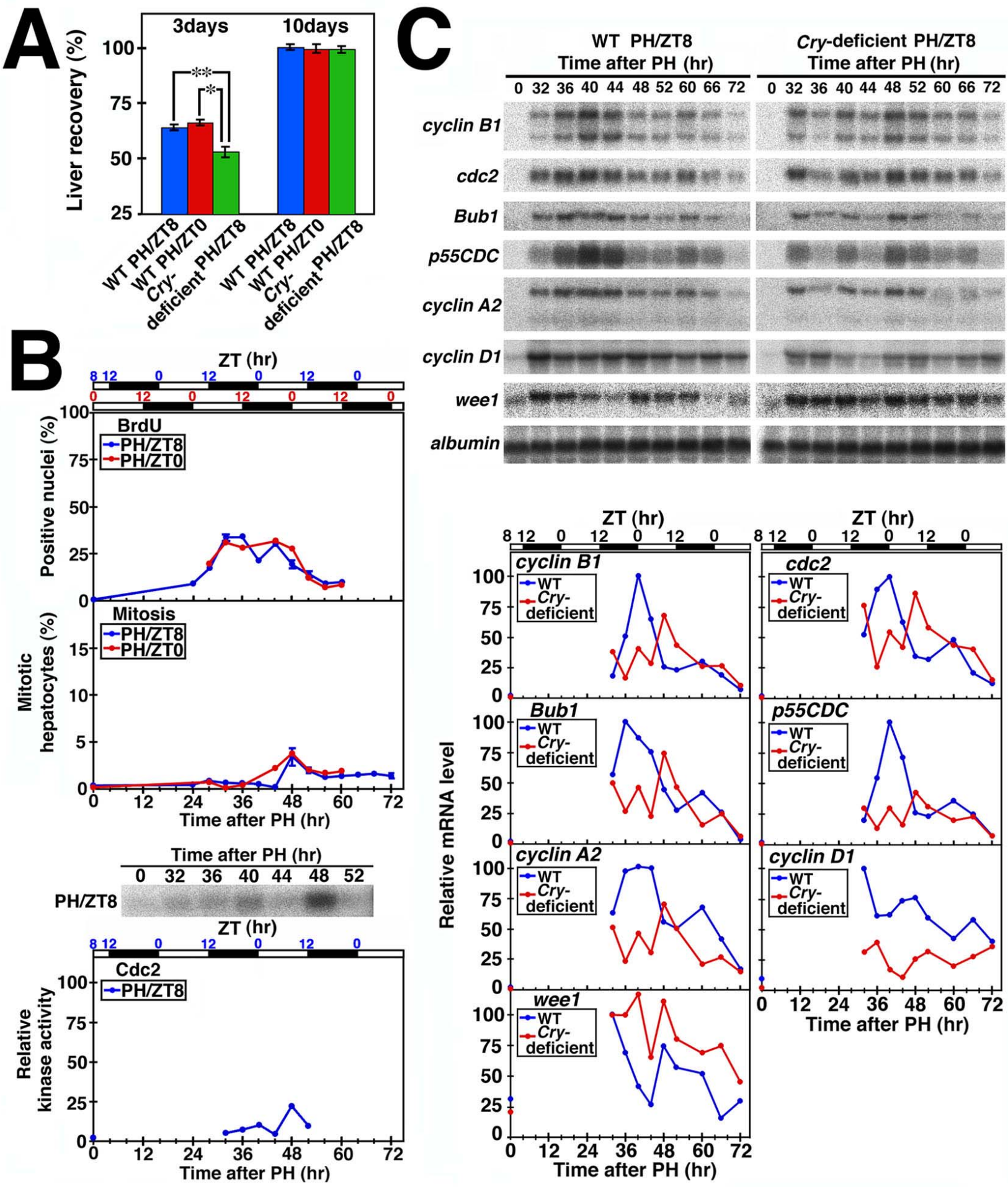
A
3days
10days
Liver recovery (%)
100
75
50
25
**
*
WT PH/ZT8
WT PH/ZT0
Cry-deficient PH/ZT8
WT PH/ZT8
WT PH/ZT0
Cry-deficient PH/ZT8
B
ZT (hr)
8 12 0 12 0 12 0
0 12 0 12 0 12 0
BrdU
PH/ZT8
PH/ZT0
Positive nuclei (%)
Mitosis
PH/ZT8
PH/ZT0
Mitotic hepatocytes (%)
Time after PH (hr)
Time after PH (hr)
0 32 36 40 44 48 52
PH/ZT8
ZT (hr)
8 12 0 12 0 12 0
Cdc2
PH/ZT8
Relative kinase activity
Time after PH (hr)
C
WT PH/ZT8
Time after PH (hr)
Cry-deficient PH/ZT8
Time after PH (hr)
0 32 36 40 44 48 52 60 66 72
cyclin B1
cdc2
Bub1
p55CDC
cyclin A2
cyclin D1
wee1
albumin
ZT (hr)
8 12 0 12 0 12 0
cyclin B1
cdc2
Bub1
p55CDC
cyclin A2
cyclin D1
wee1
WT
Cry-deficient
Relative mRNA level
Time after PH (hr)
Time after PH (hr)

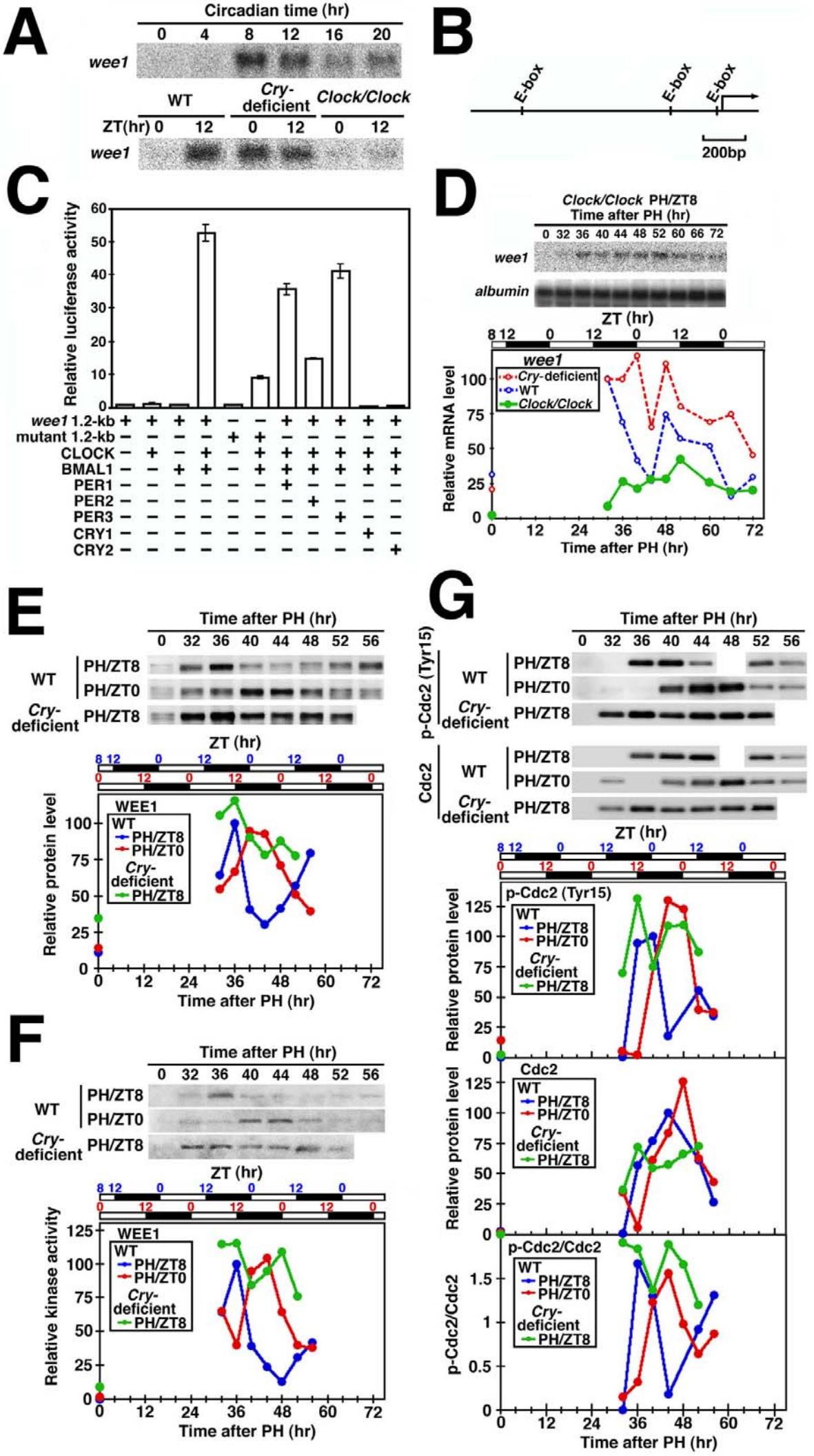
A
Circadian time (hr)
0 4 8 12 16 20
wee1
WT
Cry-deficient
Clock/Clock
ZT(hr) 0 12 0 12 0 12
wee1
B
E-box
E-box
E-box
200bp
C
Relative luciferase activity
wee1 1.2-kb
mutant 1.2-kb
CLOCK
BMAL1
PER1
PER2
PER3
CRY1
CRY2
D
Clock/Clock PH/ZT8
Time after PH (hr)
0 32 36 40 44 48 52 60 66 72
wee1
albumin
ZT (hr)
8 12 0 12 0 12 0
wee1
Cry-deficient
WT
Clock/Clock
Relative mRNA level
Time after PH (hr)
E
Time after PH (hr)
0 32 36 40 44 48 52 56
WT
PH/ZT8
PH/ZT0
Cry-deficient
PH/ZT8
ZT (hr)
WEE1
WT
PH/ZT8
PH/ZT0
Cry-deficient
PH/ZT8
Relative protein level
Time after PH (hr)
F
Time after PH (hr)
0 32 36 40 44 48 52 56
WT
PH/ZT8
PH/ZT0
Cry-deficient
PH/ZT8
ZT (hr)
WEE1
WT
PH/ZT8
PH/ZT0
Cry-deficient
PH/ZT8
Relative kinase activity
Time after PH (hr)
G
Time after PH (hr)
0 32 36 40 44 48 52 56
p-Cdc2 (Tyr15)
WT
PH/ZT8
PH/ZT0
Cry-deficient
PH/ZT8
Cdc2
WT
PH/ZT8
PH/ZT0
Cry-deficient
PH/ZT8
ZT (hr)
p-Cdc2 (Tyr15)
WT
PH/ZT8
PH/ZT0
Cry-deficient
PH/ZT8
Relative protein level
Cdc2
WT
PH/ZT8
PH/ZT0
Cry-deficient
PH/ZT8
Relative protein level
p-Cdc2/Cdc2
WT
PH/ZT8
PH/ZT0
Cry-deficient
PH/ZT8
p-Cdc2/Cdc2
Time after PH (hr)

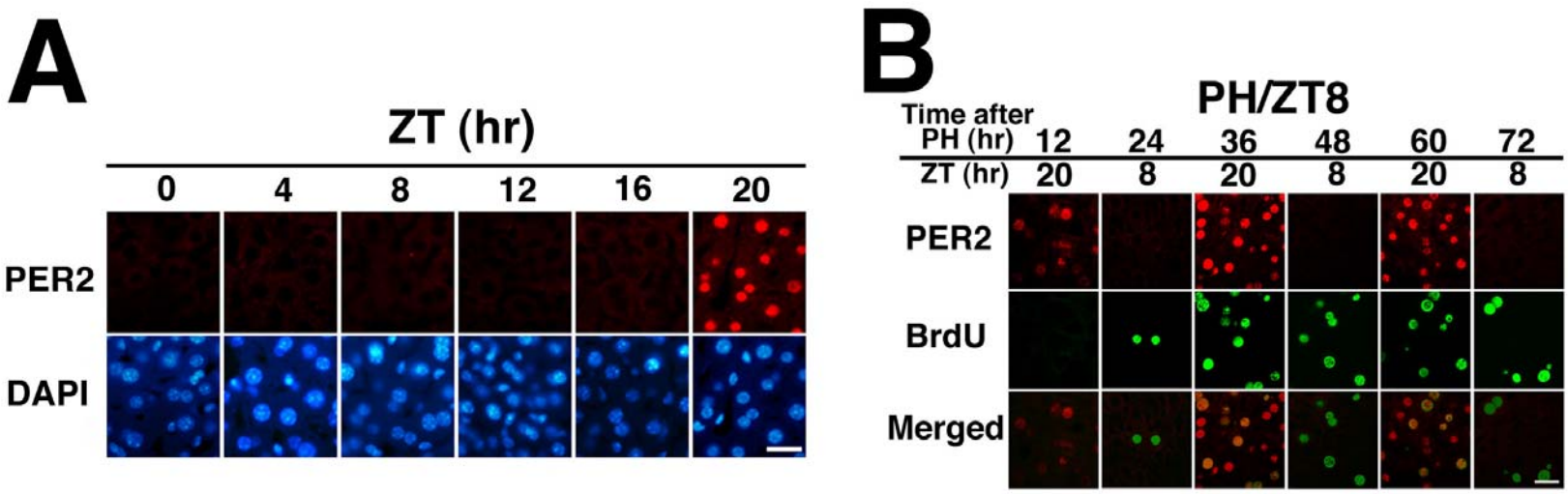
A
ZT (hr)
0
4
8
12
16
20
PER2
DAPI
B
PH/ZT8
Time after
PH (hr) 12 24 36 48 60 72
ZT (hr) 20 8 20 8 20 8
PER2
BrdU
Merged